Journal of Crystal Growth 312 (2010) 3251–3256

Contents lists available at ScienceDirect

Journal of Crystal Growth

journal homepage: www.elsevier.com/locate/jcrysgro

Impurity induced periodic mesostructures in Sb-doped SnO_2 nanowires

Annop Klamchuen [a], Takeshi Yanagida [a,b,*], Masaki Kanai [a], Kazuki Nagashima [a], Keisuke Oka [a], Tomoji Kawai [a,*], Masaru Suzuki [c], Yoshiki Hidaka [c], Shoichi Kai [c]

[a] Institute of Scientific and Industrial Research, Osaka University, 8-1 Mihogaoka, Ibaraki, Osaka 567-0047, Japan
[b] PRESTO, Japan Science and Technology Agency, 4-1-8 Honcho, Kawaguchi, Saitama 332-0012, Japan
[c] Department of Applied Quantum Physics and Nuclear Engineering, Faculty of Engineering, Kyushu University, 744 Motooka, Nishi-ku, Fukuoka 819-0395, Japan

ARTICLE INFO

Article history:
Received 24 June 2010
Received in revised form
4 August 2010
Accepted 5 August 2010
Communicated by B.A. Korgel
Available online 14 August 2010

Keywords:
A1. Crystal morphology
A1. Nanostructures
A1. Low dimensional structures
B1. Oxides

ABSTRACT

Impurity doping on semiconductor nanowires formed via vapor–liquid–solid (VLS) mechanism has been investigated with the intention being to control the transport properties. Here we demonstrate that an addition of excess impurity dopants induces a mesostructure of long range periodic arched-shape in Sb-doped SnO_2 nanowires. The microstructural and composition analysis demonstrated the importance of the presence of impurities at the growth interface during VLS growth rather than the dopant incorporation into nanowires, indicating kinetically induced mechanisms.

1. Introduction

Metal oxide nanowires formed via VLS mechanism have attracted much attention due to the nanoscale fundamental issues and also emerging nano-device applications [1] by utilizing various interesting physical properties [2–5], including resistive switching non-volatile memory effect [6–9] and ferromagnetism [10]. In general, the morphology of VLS grown oxide nanowires is a straight shape along the growth direction. Despite advances in oxide nanowire synthesis, the design and growth of hierarchical nanostructures has been limited although such controllability of nano-architectures would expand the application range of oxide nanowires. An impurity doping on VLS grown nanowires is an important process to control the transport properties, and the complex nature of dopant incorporation dynamics into nanowires has been demonstrated [11]. The major concerns as to the impurity doping on nanowires have been only directed to the relationship between the dopant incorporation and the resultant transport properties [12]. Previously we have demonstrated the dynamic effect of Sb doping on VLS grown SnO_2 nanowires [13]. Here we focus on the use of impurity doping to modify and design the morphology of VLS grown oxide nanowires. Previous studies [14,15] have demonstrated the existence of the morphology change of VLS grown Si and Ge whiskers in the presence of impurity doping with the model based on the droplet instability. However understanding the nature of the morphology change is not comprehensive due to the lack of the microstructural data. In this paper, we demonstrate the emergence of a periodic mesostructure by introducing excess Sb dopants into SnO_2 nanowires grown by VLS mechanism. Our results highlight the crucial role of kinetically induced mechanisms rather than thermodynamically stable mechanisms on the emergence of such mesostructures of VLS grown oxide nanowires.

2. Experimental

Sb-doped SnO_2 nanowires were grown on Al_2O_3 (1 1 0) oriented single crystal substrate by an Au catalyst-assisted pulsed laser deposition technique [13–16]. ArF excimer laser (Lamda-Physik COMPex 102, $\lambda=193$ nm) operating at the pulse repetition rate of 10 Hz and the laser energy of 40 mJ was used for the laser ablation [17]. The background pressure of the chamber was less than 10^{-5} Pa [18] Sn and Sb_2O_3 mixed powders were used as the target with varying the Sb dopant concentration. The Sb dopant concentration (at%) is hereafter defined as Sb/(Sb+Sn). Oxygen and argon mixed gas was introduced into the chamber with controlling the ambient total pressure 10 Pa with the ratio of oxygen and argon (1:1000) [19,20]. Prior to the laser ablation, the Au (1 nm) coated [21] Al_2O_3 substrate was preheated at the growth temperature for 20 min in the presence of pre-deposited

* Corresponding authors at: Institute of Scientific and Industrial Research, Osaka University, 8-1 Mihogaoka, Ibaraki, Osaka 567-0047, Japan.
E-mail addresses: yanagi32@sanken.osaka-u.ac.jp (T. Yanagida), kawai@sanken.osaka-u.ac.jp (T. Kawai).

0022-0248/$ - see front matter © 2010 Published by Elsevier B.V.
doi:10.1016/j.jcrysgro.2010.08.011

carbon [22]. The growth temperature was varied from 500 to 800 °C [23]. After deposition, the samples were cooled down to room temperature for 30 min. The nanowire morphology was characterized by field emission scanning electron microscopy (FESEM: Hitachi S-4300) at an accelerating voltage of 30 kV. High-resolution transmission electron microscopy (HRTEM: JEOL JEM-3000F) coupled with energy dispersive spectroscopy (EDS) at an accelerating voltage of 300 kV was used to evaluate the diameter, the crystallinity and the composition of the fabricated nanowires. Scanning transmission electron microscopy (STEM: Hitachi HD-2700) at an accelerating voltage of 200 kV was used to clarify the local composition of the nanowires. The growth rate, size and periodicity of nanowires were analyzed by averaging the data for 500 samples in microscopy images for statistical reliability. The probing size was approximately 0.4 nm. X-ray diffraction (XRD) and the reciprocal space mapping (RSM) were performed to identify crystal structures of nanowires.

3. Results and discussion

Fig. 1(a) and (b) shows the FESEM images of fabricated Sb-doped SnO_2 nanowires grown on Al_2O_3 single crystal substrate when varying the dopant concentrations of source. The straight-shaped nanowires can be seen for relatively low dopant concentration 5 at%, whereas the mesostructures emerged for 20 at% case. The arched-shape mesostructures have a long range periodicity of 200 ± 25 nm. This length scale was not likely to be dependent on the impurity concentration in the supplying source. HRTEM analysis demonstrated the presence of metal catalysts at the tip in both dopant concentrations, indicating the occurrence of VLS nanowire growth via metal catalysts [24]. The crystallinity of fabricated nanowires and the presence of Sb within nanowires were examined by XRD and HRTEM-EDS, as shown in Fig. 1(c) and (d). These results confirmed the presence of Sb dopants within single crystalline SnO_2 nanowires. Thus introducing excess Sb impurity dopants during SnO_2 VLS growth resulted in a mesostructure of oxide nanowires.

Fig. 2(a) shows the diagram as to the emergence of such mesostructures when varying both the growth temperature and the Sb concentrations of source. The arched-shape mesostructures of nanowires appeared above 10 at% of the dopant concentrations of source and above 700 °C of the growth temperature. Here we question the mechanism to explain the emergence of mesostructures. The most natural scenario is based on the dopant incorporation into nanowires. Thus we examined the dopant concentration incorporated into nanowires by HRTEM-EDS, as shown in Fig. 2(b). It can be seen that the incorporated dopant concentration was limited around 2–3 at% even increasing the dopant concentrations of source. This indicates the occurrence of re-evaporation events of Sb during VLS growth [13]. Thus the dopant incorporation into nanowires alone cannot explain the emergence of mesostructures.

Fig. 2(b) also shows the growth rate of nanowires when varying the dopant concentration of source. The growth ate increased when there is an increase in the dopant concentrations of source, and then saturated at around 10 at%. The increase in the growth rate of nanowires and the re-evaporation events

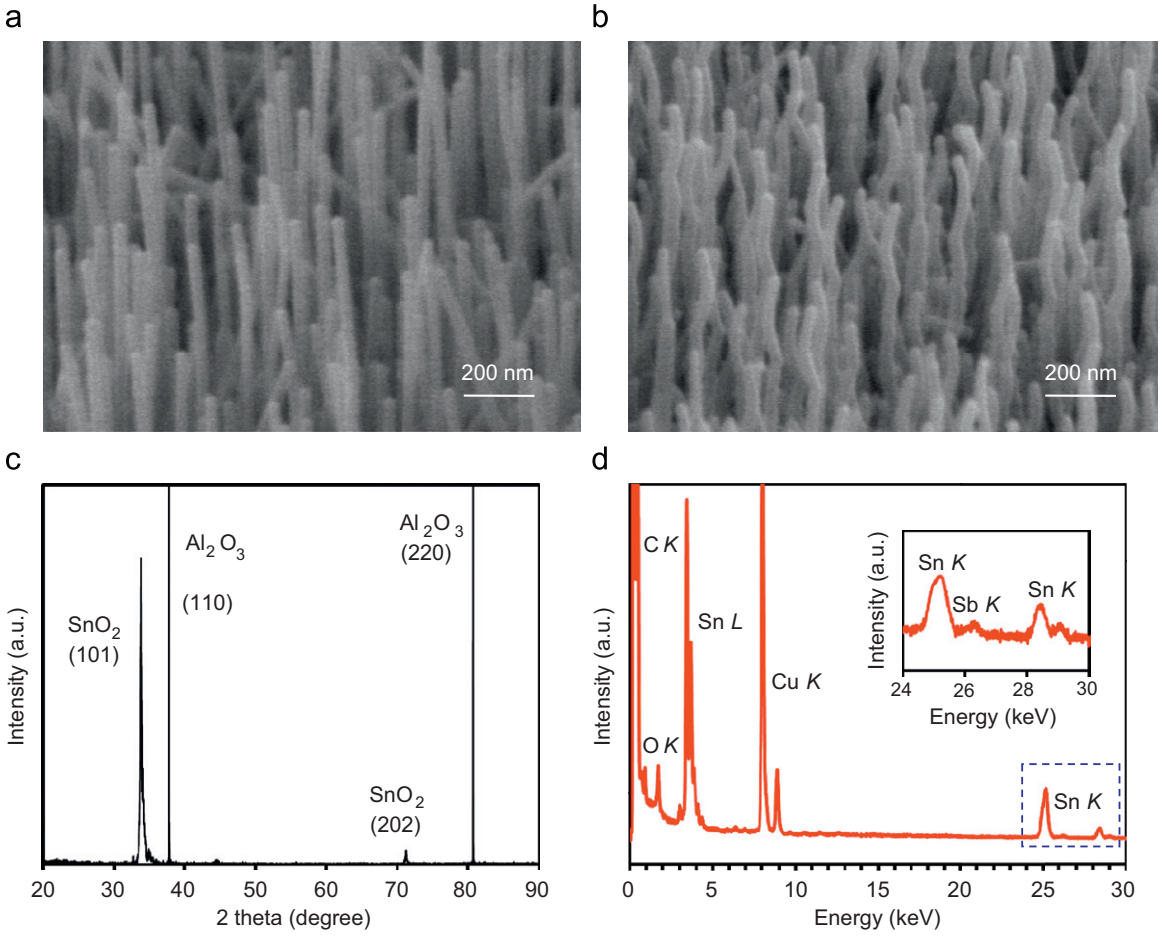

Fig. 1. (a) and (b) shows the FESEM images of fabricated Sb-doped SnO_2 nanowires when varying the Sb dopant concentrations in supplied source. (a) 5 at% and (b) 20 at%, respectively. (c) XRD data and (d) EDS data of Sb-doped SnO_2 nanowires.

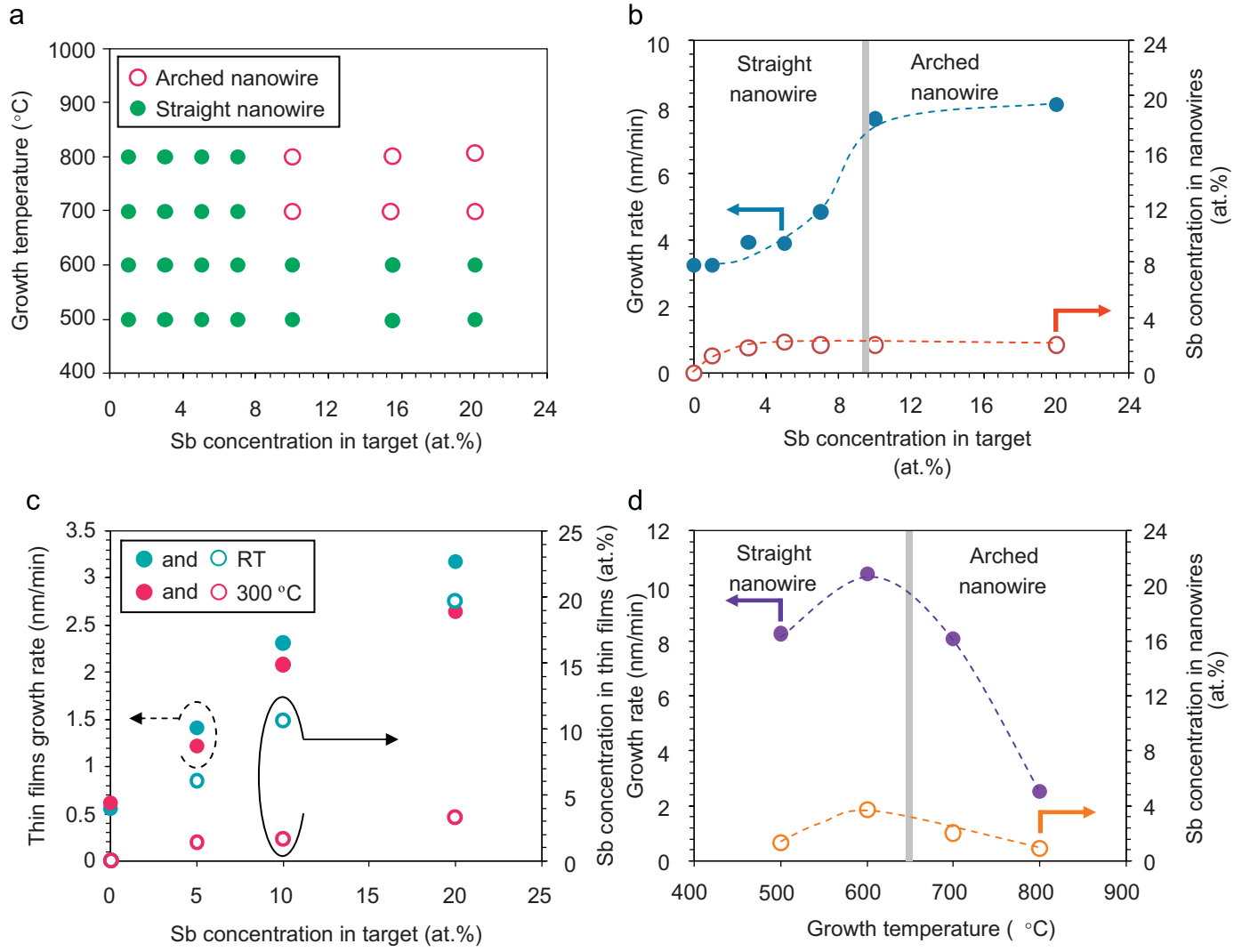

Fig. 2. (a) Diagram as to the emergence of nanowire mesostructures when varying both the growth temperature and the Sb dopant concentration in source. Open circles show the nanowire mesostructures and closed circles show the straight nanowires. (b) Growth rate (left *y*-axis) and the dopant concentration incorporated into nanowires (right *y*-axis) of Sb-doped SnO_2 nanowires when varying the Sb dopant concentrations in source. (c) Growth rate (left *y*-axis) and the dopant concentration incorporated (right *y*-axis) of Sb-doped SnO_2 thin films when varying the Sb dopant concentrations in source. The thin films used here were fabricated at room temperature or 300 °C. (d) Growth rate (left *y*-axis) and the dopant concentration incorporated into nanowires (right *y*-axis) of Sb(20 at%)-doped SnO_2 nanowires when varying the growth temperature.

of Sb were also confirmed in the thin film experiments as shown in Fig. 2(c). The increase in growth rate with increase in the dopant concentrations of source, can be interpreted in terms of the increase in impinging flux. Although there seems to be a correlation between the growth rate and the emergence of mesostructures, such correlation did not exist when varying the growth temperature as shown in Fig. 2(d), where the mesostructures appeared when the growth rate decreased above 700 °C of growth temperature. Thus these experimental results highlight that the growth rate effects alone cannot explain the emergence of mesostructures. There are other several possible scenarios. The incorporated impurity dopant might modify the crystal structures of SnO_2 nanowires. The induced crystal distortion or imperfections might cause the mesostructures. To address this issue, we have performed RSM measurements to identify the crystal structures when doping. Fig. 3(a)–(c) shows the RSM data around (3 0 1) and 2θ scan data (ω was fixed to be 3.19°) of straight-shaped and mesostructured SnO_2 nanowires. These data do not show any significant discrepancies between straight-shaped and mesostructured SnO_2 nanowires on the crystal structures, since the lattice constants and the full-width half maximum (FWHM) were found to be similar for both cases. The nanowire mesostructures showed broader peak rather than non-doped nanowires within in-plane, this is due to the variations of nanowire growth direction. In addition, HRTEM analysis around the kink of the mesostructures demonstrates the absence of any observable crystal dislocations Fig. 3(d). Thus the scenario based on the modification of crystal structures alone cannot explain the emergence of the mesostructures. Above results demonstrate that mechanisms based on thermodynamically stable structures are not appropriate to interpret the emergence of mesostructures, indicating possibly kinetically induced mechanisms. The presence of Sb impurity dopants around the growth interface might affect the VLS growth kinetics via modifying the precipitation events from metal catalysts. Since the liquid–solid interface of metal catalysts is responsible for VLS nanowire formation, the presence of impurity at the growth interface might modify the growth mode.

Fig. 4 shows the STEM images around the tip of Sb-doped SnO_2 nanowires. Sb was found to exist mainly around the metal

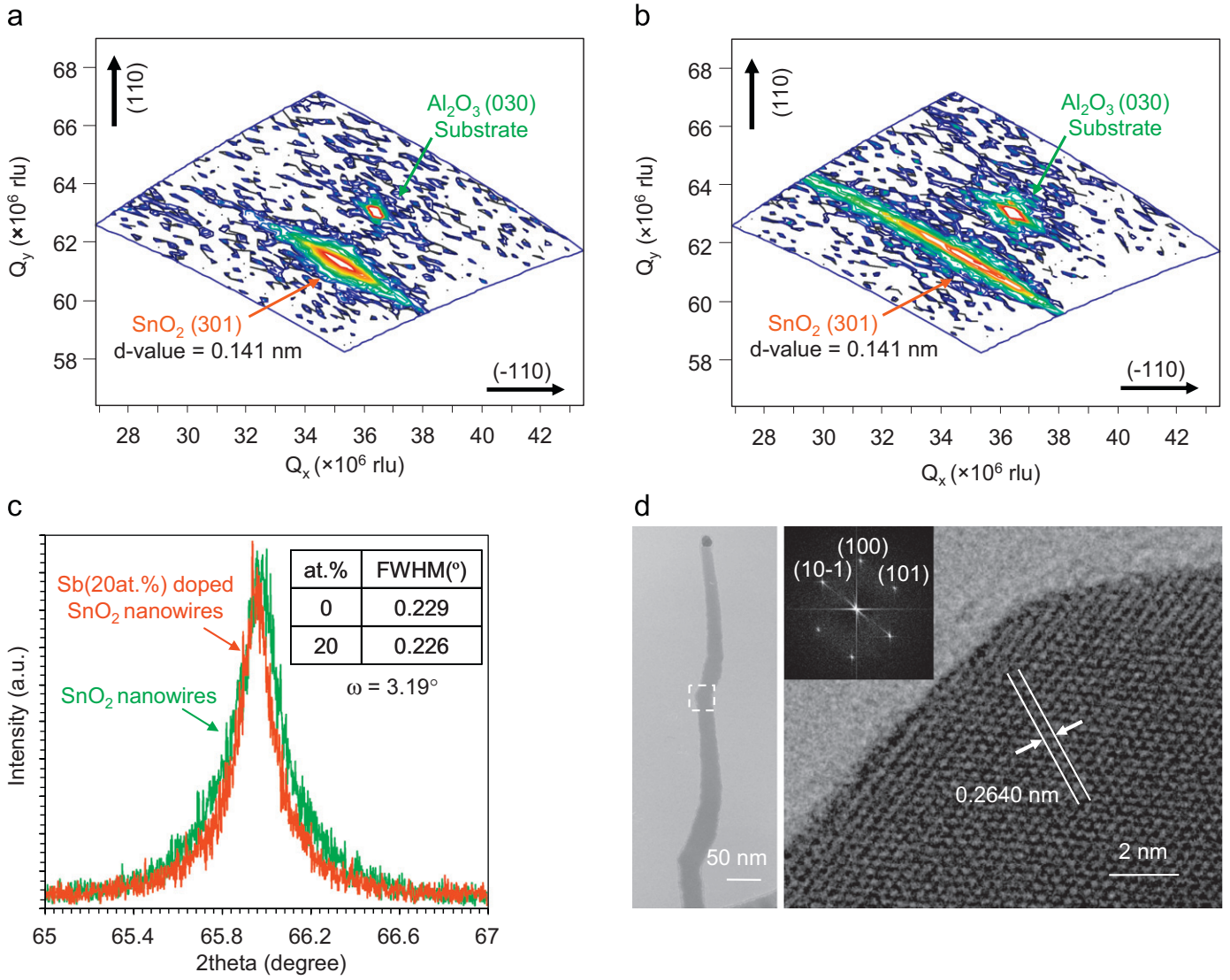

Fig. 3. (a) RSM data of non-doped SnO_2 nanowires performed around the (3 0 1) peak. (b) RSM data of Sb(20 at%)-doped SnO_2 nanowires performed around the (3 0 1) peak. (c) 2θ scan data of both non-doped and Sb(20 at%)-doped SnO_2 nanowires. ω value was fixed to be 3.19°. Inset table shows the FWHM data. (d) HRTEM images of Sb-doped SnO_2 nanowire mesostructure. Left shows the overview image and right shows the magnified image of the kink. Inset shows the two dimensional fast Fourier transform pattern.

catalyst rather than the inside of nanowires. In fact, the low concentration of Sb incorporated into nanowires is consistent with the previous EDS results in Fig. 1(d). The presence of excess impurity dopants around the growth interface during VLS growth seems to be responsible for the emergence of observed mesostructures. The surface energy of droplet (α_{LS} and α_{VL}) and the corresponding surface tension (γ_{LS} and γ_{VL}) might be modified by the adsorption of the impurity dopant. When the γ_{LS} increases and/or the γ_{VL} decreases, the droplet is destabilized due to the less wettability of the droplet, which has been reported in previous studies [14,15,25]. Givargizov [14] reported the role of vapor doping ($AsCl_3$ doped Si and Ge whisker) which might modify the surface energy (α_{LS} and α_{VL}) or the corresponding surface tension (γ_{LS} and γ_{VL}) of droplet due to the adsorption of the impurity and shown the result of periodic instability of Si and Ge whisker. Moreover recently, Algra et al. [15] have reported the periodic twinning of InP induced by doping Zn impurity during VLS growth, which was discussed in terms of the difference between the liquid–solid contact angle and the tilt angle of the external facet of the nucleus. From the viewpoint of surface energy modification model, it can be assumed that the droplet size, i.e., L–S interface size decreases with increase in the dopant concentration in target source. Fig. 5 shows the Sb dopant concentration dependent on the droplet size. This shows that the droplet size decreased with increase in the dopant concentration. These results highlight that long range periodic mesostructures are possibly due to the modification of the surface energy of catalyst droplets. Although the direct experimental evidences as to the modulations of the contact angle of catalyst droplets are crucial to justify the instability of VLS growth around the growth interface in this work, this would be an interesting future work by performing *in-situ* TEM experiments. This mechanism is rather dynamic since the flux of impurity dopants across the growth interface rather than the dopants remained within nanowires alone contributes the emergence of the mesostructures. In other words, the instability of VLS growth around the growth interface was induced by excess impurity dopants. Such instability induced periodic structures were well known and commonly observed in nature to create hierarchical structures via so-called "energy dissipative processes" [26–32]. Although the real time *in situ*

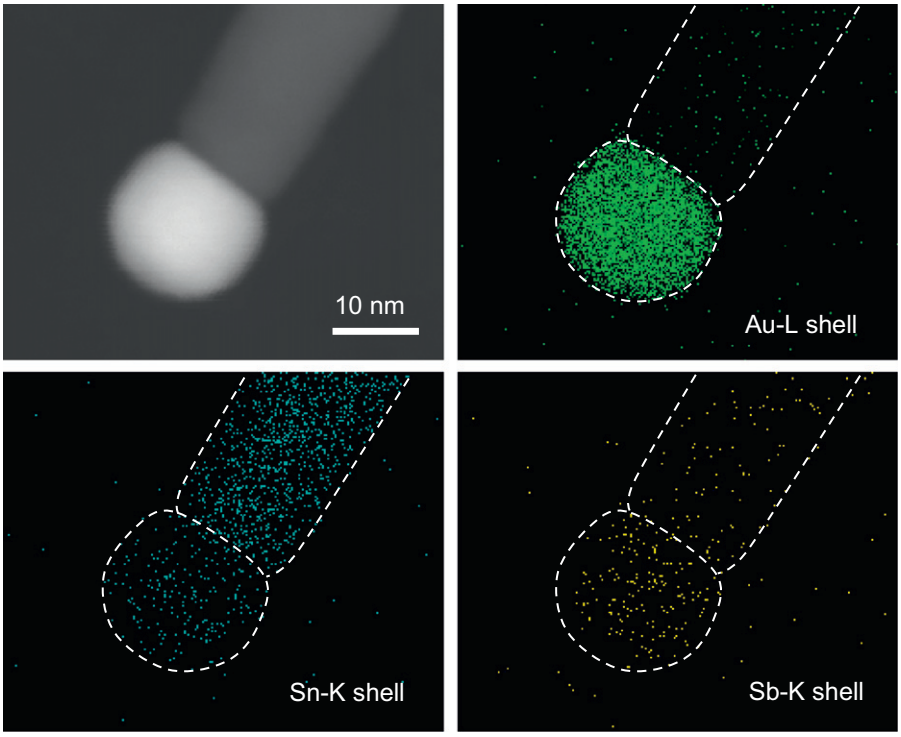

Fig. 4. STEM image and elemental mapping images (Au, Sn and Sb) of Sb(20 at%)-doped SnO_2 nanowires.

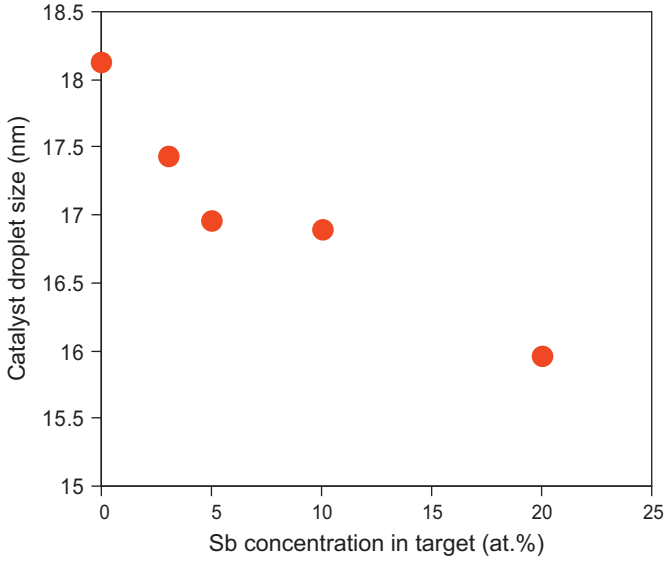

Fig. 5. Variation of catalyst droplet sizes when varying the Sb impurity concentration in the supplying source.

experimental observations need to be undertaken, our results consistently demonstrated the importance of kinetically induced mechanisms.

4. Conclusion

In summary, we have demonstrated that an addition of excess impurity dopants induces a mesostructure in Sb-doped SnO_2 nanowires. The microstructural analysis demonstrated the importance of the presence of impurities around the growth interface on the emergence of such mesostructures rather than the dopant incorporation into nanowires, indicating kinetically induced mechanism.

Acknowledgments

This study was in part supported by a Grant-in-Aid for Scientific Research on Innovative Areas [20111004] from the Ministry of Education, Culture Sports, Science and Technology (MEXT) of Japan. T.K was partly supported by FIRST program.

References

[1] I. Hochbaum, R. Chen, R.D. Delgado, W. Liang, E.C. Garnett, M. Najarian, A. Majumdar, P.D. Yang, Nature 451 (2008) 163.
[2] Y. Tomioka, A. Asamitsu, Y. Moritomo, H. Kuwahara, Y. Tokura, Phys. Rev. Lett. 74 (1995) 5108.
[3] B.S. Kwak, A. Erbil, B.J. Wilkens, J.D. Budai, M.F. Chisholm, L.A. Boatner, Phys. Rev. Lett. 68 (1992) 3733.
[4] J.P. Locquet, J. Perret, J. Fompeyrine, E. Mäechler, J.W. Seo, G. Van Tendeloo, Nature 394 (1998) 453.
[5] M.I.S. Faley, B. Mi, A. Petraru, C.L. Jia, U. Poppe, K. Urban, Appl. Phys. Lett. 89 (2006) 082507.
[6] K. Nagashima, T. Yanagida, K. Oka, T. Kawai, Appl. Phys. Lett. 94 (2009) 242902.
[7] K. Oka, T. Yanagida, K. Nagashima, H. Tanaka, T. Kawai, J. Am. Chem. Soc. 131 (2009) 3434.
[8] K. Nagashima, T. Yanagida, K. Oka, M. Taniguchi, T. Kawai, J.S. Kim, B.H. Park, Nano Lett. 10 (2010) 1359.
[9] K. Oka, T. Yanagida, K. Nagashima, T. Kawai, J.S. Kim, B.H. Park, J. Am. Chem. Soc. 132 (2010) 6634.
[10] A. Marcu, T. Yanagida, K. Nagashima, K. Oka, H. Tanaka, T. Kawai, Appl. Phys. Lett. 92 (2008) 173119.
[11] E.C. Garnett, Y.C. Tseng, D.R. Khanal, J. Wu, J. Bokor, P.D. Yang, Nat. Nanotechnol. 4 (2009) 311.
[12] D.E. Perea, E.R. Hemesath, E.J. Schwalbach, J.L. Lensch-Falk, P.W. Voorhees, L.J. Lauhon, Nat. Nanotechnol. 4 (2009) 315.
[13] A. Klamchuen, T. Yanagida, K. Nagashima, S. Seki, K. Oka, M. Taniguchi, T. Kawai, Appl. Phys. Lett. 95 (2009) 053105.
[14] E.I. Givargizov, J. Cryst. Growth 20 (1973) 217.
[15] R.E. Algra, M.A. Verheijen, M.T. Borgström, L.-F. Feiner, G. Immink, W.J.P. van Enckevort, E. Vlieg, E.P.A.M. Bakkers, Nature 456 (2008) 369.
[16] K. Nagashima, T. Yanagida, H. Tanaka, T. Kawai, J. Appl. Phys. 101 (2007) 124304.

[17] A. Marcu, T. Yanagida, K. Nagashima, H. Tanaka, T. Kawai, J. Appl. Phys. 102 (2007) 016102.
[18] K. Nagashima, T. Yanagida, H. Tanaka, T. Kawai, Appl. Phys. Lett. 90 (2007) 233103.
[19] T. Yanagida, K. Nagashima, H. Tanaka, T. Kawai, Appl. Phys. Lett. 91 (2007) 061502.
[20] K. Nagashima, T. Yanagida, K. Oka, H. Tanaka, T. Kawai, Appl. Phys. Lett. 93 (2008) 153103.
[21] T. Yanagida, K. Nagashima, H. Tanaka, T. Kawai, J. Appl. Phys. 104 (2008) 016101.
[22] T. Yanagida, A. Marcu, H. Matsui, K. Nagashima, K. Oka, K. Yokota, M. Taniguchi, T. Kawai, J. Phys. Chem. C. 112 (2008) 18923.
[23] K. Nagashima, T. Yanagida, A. Klamchuen, M. Kanai, K. Oka, S. Seki, T. Kawai, Appl. Phys. Lett. 96 (2010) 073110.
[24] R.S. Wagner, W.C. Ellis, Appl. Phys. Lett. 4 (1964) 89.
[25] J. Westwater, D.P. Gosain, S. Tomiya, S. Usui, J. Vac. Sci. Technol. B 15 (1997) 554.
[26] S. Mann, Nat. Mater. 8 (2009) 781.
[27] K.V. Tretiakov, K.J.M. Bishop, B.A. Grzybowski, J. Phys. Chem. B 113 (2009) 7574.
[28] H. Liu, E.D. Spoerke, M. Bachand, S.J. Koch, B.C. Bunker, G.D. Bachand, Adv. Mater. 20 (2008) 4476.
[29] S.A. Beznosyuk, A.V. Kolesnikov, D.A. Mezentsev, M.S. Zhukovsky, T.M. Zhukovsky, Mater. Sci. Eng. C 19 (2002) 91.
[30] B. Tian, P. Xie, T.J. Kempa, D.C. Bell, C.M. Lieber, Nat. Nanotechnol. 4 (2009) 824.
[31] C. Sanchez, H. Arribart, M.M.G. Guille, Nat. Mater. 4 (2009) 277.
[32] H. Chu, X. Li, G. Chen, Z. Jin, Y. Zhang, Y. Li, Nano Res. 1 (2008) 213.